Applied Radiation and Isotopes 115 (2016) 235–250

Contents lists available at ScienceDirect

Applied Radiation and Isotopes

journal homepage: www.elsevier.com/locate/apradiso

Study on patient-induced radioactivity during proton treatment in hengjian proton medical facility

Qingbiao Wu [a,b,*], Qingbin Wang [a,b], Tianjiao Liang [b,c], Gang Zhang [a,b], Yinglin Ma [a,b], Yu Chen [a,b], Rong Ye [a,b], Qiongyao Liu [a,b], Yufei Wang [a,b], Huaibao Wang [a,b]

[a] China Spallation Neutron Source (CSNS), Institute of High Energy Physics (IHEP), Chinese Academy of Sciences (CAS), Dongguan 523803, People's Republic of China
[b] Dongguan Institute of Neutron Science (DINS), Dongguan 523808, People's Republic of China
[c] China Spallation Neutron Source (CSNS), Institute of Physics (IPHY), Chinese Academy of Sciences (CAS), Dongguan 523803, People's Republic of China

HIGHLIGHTS

- A detailed study on patient-induced radioactivity was conducted by adopting Monte Carlo code FLUKA and activation formula.
- New formulas for calculating the activity build-up process of periodic irradiation were derived and extensively studied.
- Patient induced radioactivity, which has been ignored for years, is confirmed as a vital factor for radiation protection.
- The induced radioactivity from single short-time treatment and long-time running (saturation) were studied and compared.
- Some suggestions on how to reduce the hazard of patient's induced radioactivity were given.

ARTICLE INFO

Article history:
Received 19 December 2015
Received in revised form
16 June 2016
Accepted 27 June 2016
Available online 28 June 2016

Keywords:
Induced radioactivity
Patient
Proton
FLUKA
dose
Activation
O-15
Buildup
Saturation degree

ABSTRACT

At present, increasingly more proton medical facilities have been established globally for better curative effect and less side effect in tumor treatment. Compared with electron and photon, proton delivers more energy and dose at its end of range (Bragg peak), and has less lateral scattering for its much larger mass. However, proton is much easier to produce neutron and induced radioactivity, which makes radiation protection for proton accelerators more difficult than for electron accelerators. This study focuses on the problem of patient-induced radioactivity during proton treatment, which has been ignored for years. However, we confirmed it is a vital factor for radiation protection to both patient escort and positioning technician, by FLUKA's simulation and activation formula calculation of Hengjian Proton Medical Facility (HJPMF), whose energy ranges from 130 to 230 MeV. Furthermore, new formulas for calculating the activity buildup process of periodic irradiation were derived and used to study the relationship between saturation degree and half-life of nuclides. Finally, suggestions are put forward to lessen the radiation hazard from patient-induced radioactivity.

1. Introduction

At present, increasingly more proton medical facilities have been established globally for better curative effect and less side effect in tumor treatment. Compared with photon and electron, proton delivers more energy and dose at its end of range (Bragg peak), and has less lateral scattering for its much larger mass. However, proton is much easier to produce neutron and induced radioactivity, when energy is scaled up to several million electron volts, which makes radiation protection for proton accelerators more difficult than for electron accelerators. This study focuses on the problem of patient-induced radioactivity during proton treatment, which has been ignored for years. However, it has been extensively studied by the author in the process of radiation protection design for Hengjian Proton Medical Facility (HJPMF).

HJPMF is planned to be built in Guangzhou, Guangdong, China, with its proton accelerator named C230 cyclotron bought from IBA (one of the famous proton medical facility producers). As shown in Fig. 1, in HJPMF, degrader, collimator, and slits form the energy selection system (ESS) and both cyclotron and ESS are located in the cyclotron room. First, 230-MeV proton beam is extracted from the C230 cyclotron, then the beam's energy is degraded from

* Corresponding author.

http://dx.doi.org/10.1016/j.apradiso.2016.06.029
0969-8043/

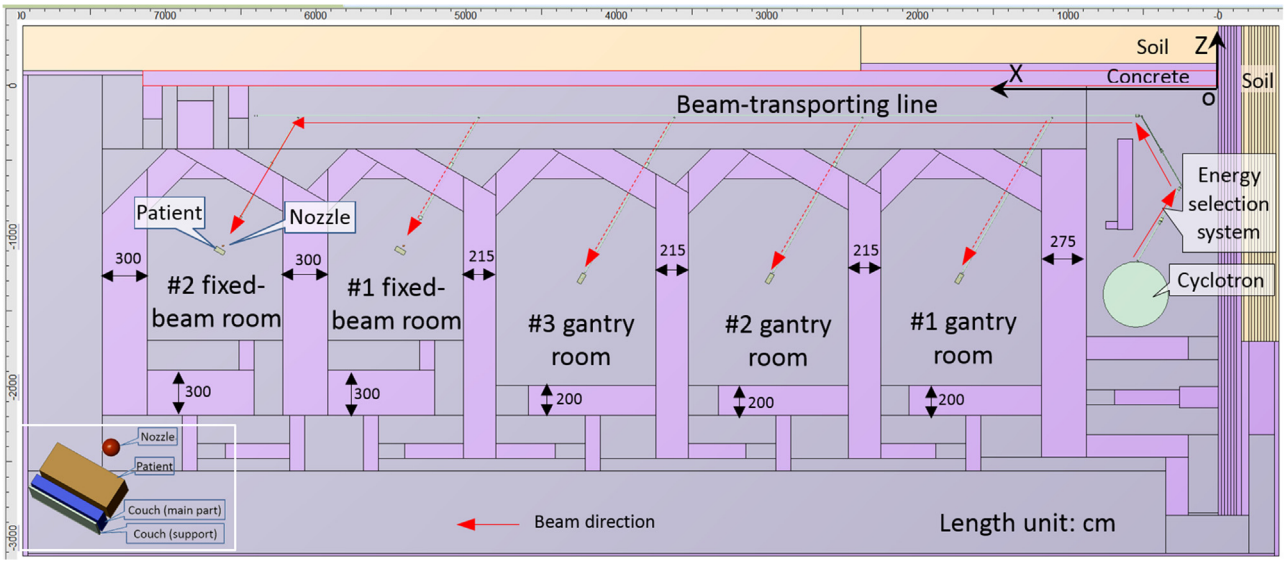

Fig. 1. Structure of HJPMF at its beam plane, plotted using SimpleGeo (details of components distribution in fixed-beam room shown at the lower left corner) (Theis et al., 2006).

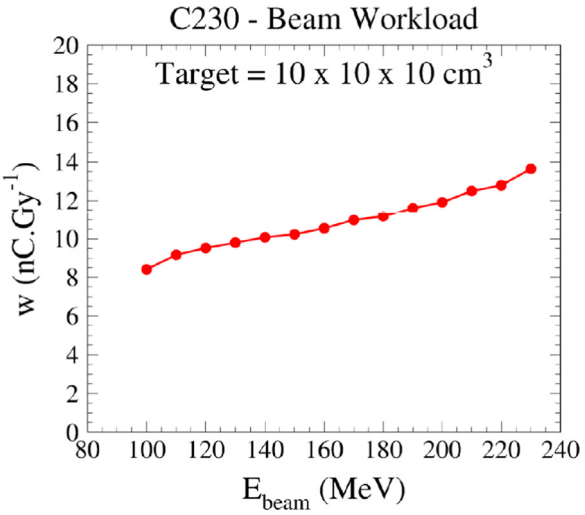

Fig. 2. Beam workload as a function of beam energy to deliver 1-Gy dose in a 1-L water target volume (Stichelbaut, 2014a, b).

230 MeV to a certain energy between 130 and 230 MeV by the degrader. The beam is then collimated and size-reduced by the collimator and slits. Afterward, the beam is transported to the beam-transporting line (BTL), turned to the treatment room, and allowed to reach the target (patient) (Stichelbaut, 2014a). Only pencil beam scanning (PBS) mode will be adopted for treatment in HJPMF, to avoid beam loss at nozzle and aperture. Only two source terms need to be considered from BTL to patient: beam line loss at beam pipe with most 0.106 nA at 230 MeV and beam point loss at patient with most 1.66 nA at 230 MeV. In HJPMF, five treatment rooms are planned, including three gantry rooms and two fixed-beam rooms. During treatment, the beam transports from BTL to one of the treatment rooms; the other rooms have no beam and are prepared for patient positioning. The proton energy is also changeable to adapt to different tumor depths. In IBA's treatment assumption (Stichelbaut, 2014a, b), 350 patients were treated every year and in each room, and 4800 h per year are spent for treatment (16 h/day, 6 days/week, 50 weeks/year). Fig. 2 shows the beam workload (expressed in nanocoulombs) needed to deliver 1-Gy dose in 1 L of water (note: patient can be replaced by water phantom). IBA also listed the possible clinical indications through

Table 1
Beam energy, workload weight, IBA workload and HJPMF workload obtained with IBA case mix (Stichelbaut, 2014b).

Energy (MeV)	230	210	180	160	130	Total
IBA workload per room (nA.h)	37.25	29.59	26.08	66.34	52.5	211.76
Workload weight	0.176	0.140	0.123	0.313	0.248	1.000
HJPMF workload per room (nA.h)	88.00	70.00	61.50	156.50	124.00	500.00

the running experiences from its approximately 20 proton treatment centers (Stichelbaut, 2014b). Combining the workload with the possible clinical indications, and according to the five energy points used in HJPMF, IBA converted the case mix into annual workloads, as shown in rows 1–3 in Table 1. Referring to these IBA's treatment assumptions and the five energy points' workload weight presented in Table 1, HJPMF established its treatment annual workloads as shown in Table 2 and the corresponding energy workload as shown in Table 1.

According to Tables 1 and 2, and combined with the transporting efficiency in ref. Stichelbaut (2014a), we obtained all the source terms in HJPMF, whose source terms in each treatment room are shown in Table 3. Some notes in our calculation are also shown in Table 3.

The dose-governed target values for HJPMF are 5 and 0.1 mSv/a for radiation worker and public, respectively. The dose rate limit is <2.5 μSv/h in the working place for shielding design, and the designed structure is shown in Fig. 1.

2. Calculation and analysis

2.1. Geometrical model and calculation method

In order to calculate induced radioactivity in the treatment room of HJPMF, Monte Carlo code FLUKA (Ferrari et al., 2011; Bohlen et al., 2014) was adopted to simulate the beam loss and transport process. The geometrical model shown in Fig. 1 was plotted using SimpleGeo (Theis et al., 2006). In order to simplify and consider the components' activation, all the magnets and other components were omitted, except beam pipe, nozzle, patient, and walls. The beam pipe was constructed as a cylindrical shell made of pure iron material, with inner and outer radii 4 and

Table 2
Annual workload of HJPMF obtained by referring to IBA.

Patients per day	Fields per patient	Time per field (min)	Beam current (nA)	Daily workload per patient (nA.h)	Daily workload per room (nA.h)	Annual workload per room (treatment) (nA.h)	Annual workload per room (QA) (nA.h)	Annual workload per room (total) (nA.h)	Number of treatment rooms
30	2	1.00	1.00	0.03	1.00	300.00	200.00	500.00	5

5 cm, respectively. The nozzle was constructed as a sphere made of copper, with radius 8 cm. The patient was replaced by a rectangular water phantom with dimensions $30 \times 30 \times 70$ cm (the same size of human chest, referred by Mukherjee's report) (Mukherjee, 2009). The concrete wall was constructed according to its true size, with the material adopted from FLUKA manual (Ferrari et al., 2011). For comparison, two situations of with and without couch were considered. For convenience of simulation, in accordance with IBA (Stichelbaut, 2014a), couch was assumed located in the #2 fixed-beam room, behind the patient along the proton beam direction, with the same cross section as the patient, but its main part is made of 10-cm-thick polyethylene and its support made of 2-cm-thick stainless steel 304. The details of component distribution in the fixed-beam room are shown in Fig. 1. The components and element compositions are listed in Table 4.

During treatment, the position of the patient is fixed on the couch at the isocenter, and proton beam emits from the nozzle and reaches the patient. The treatment in gantry room is characterized by 360° rotation of nozzle around the patient to change the position, whereas the position is fixed in the fixed-beam room. Therefore, in our simulation in the gantry room, the proton was sampled uniformly from a circle just around the patient and emitted toward the circle's center (also concentric to the patient); however, in the fixed-beam room, the proton was sampled between the nozzle and patient, and emitted toward the patient directly. In the calculation, we assumed the air ventilation frequency is one time per hour.

2.2. Number of treatment rooms, patients per day, and time per patient

As shown in Table 2, in the treatment room, 30 patients are to be treated in 16 h per day, with two fields per patient during each treatment and with 1 min per field. This indicates that the beam hits the patient for only 2 min in each 32-min treatment. The other 30 min are free of beam and are used for patient posture and position. To simplify, we assumed the two fields are continuous, and no need for positioning technician entering the treatment room for the second field reposition.

Therefore, the 2-min running and 30-min cooling processes must be simulated to consider the short-time treatment-induced radioactivity. With more treatments conducted, the induced radioactivity will build up and finally reach saturation. In the treatment room, single short-time activation will dominate at the beginning. However, after long-time running, saturation radioactivity may dominate. Therefore, long-time saturation activation must be calculated and compared with single short-time activation.

We also realized that the patient might produce induced radioactivity as other components such as beam pipe, nozzle, air, concrete wall, and couch. The patient will become a radiation source to his/her surrounding environment and produce some radiation to his/her escort and positioning technician. Therefore, the strength and influence of the patient-induced radioactivity must be analyzed as well.

2.3. Simulation techniques

In order to calculate the residual dose rate and radionuclides from patient and air, the single short-time irradiation profile of 2-min treatment with different cooling time (1 min, 5 min, 10 min, 30 min, 1 h, 4 h, 1 day, and 1 week) was simulated. For calculation of long-time saturation activity, we assumed the life-time of HJPMF as 30 years, and the long-time irradiation profile of 30-year continuous treatment (without beam cut off time) with the same beam energy and current as the single 2-min treatment was simulated. In order to distinguish the residual dose rate of each component (especially "patient" and "concrete"), a "two-step simulation" method was adopted. For example, at the first step of simulation, we set concrete to "black hole" to stop the secondary

Table 3
Source: Source terms in each treatment room of HJPMF.

Source term	Proton energy (MeV)	Proton loss rate (%)	Loss workload (nA.h)	Target material	Loss frequency	Annual loss time (h)	Loss beam current (nA)	Annual workload per room (nA.h)
Beam line point (average)+ Beam line distributed	230	6	5.6	Fe	Continuous when beam on	53.08	0.106	31.91
	210		4.5			59.37	0.075	
	180		3.9			95.39	0.041	
	160		10.0			303.41	0.033	
	130		7.9			448.75	0.018	
Beam line point (peak)	230	100	0.122	Fe	5 s/day@1 d/week	0.07	1.76	0.32
	210		0.087				1.25	
	180		0.048				0.69	
	160		0.038				0.55	
	130		0.020				0.29	
Patient (PBS mode)	230	100	88.00	Tissue	Continuous when beam on	53.08	1.66	500.00
	210		70.00			59.37	1.18	
	180		61.50			95.39	0.64	
	160		156.50			303.41	0.52	
	130		124.00			448.75	0.28	

Note: (1) During treatment, instant beam current fluctuates around average beam current, the peak current is ~8 nA, but the average beam current controlled is no more than 1.66 nA; (2) The highest energy 230 MeV with the biggest beam current of all the energy points was adopted for the conservative calculations; (3) The source term "beam line point (peak)" was omitted in the calculation, as its workload is 2–4 orders of magnitude lower than other two source terms and difficult to determine the loss point.

Table 4
Components and element compositions in treatment room.

Component	Density (g/cm^3)	Element composition	Mass fraction (%)	Element composition	Mass fraction (%)
Beam pipe (iron)	7.874	Fe	100		
Nozzle (copper)	8.96	Cu	100		
Air	0.001225	N	75.558	O	23.159
		Ar	1.2832		
Concrete wall	2.35	H	1.000	C	0.1
		O	52.9107	Na	1.6
		Mg	0.2	Al	3.3872
		Si	33.7021	K	1.3
		Ca	4.4	Fe	1.4
Couch (polyethylene)	0.92	H	4.03	C	95.97
Couch (steel 304)	7.93	C	0.07367	Si	1.0524
		Mn	2.1048	Cr	17.8910
		Ni	8.4193	S	0.0316
		P	0.0368	Co	1.0E-05
		Fe	70.3904		
Patient (water phantom)	1	H	11.19	O	88.81

particles at the boundary to obtain the result without concrete and written the boundary-crossing particles' information into a file; at the second step of simulation, we read the file as source term to continue the particles' transport in concrete and obtain the result from concrete.

2.4. Induced dose rate distribution and its decay with time

Fig. 3 shows the dose rate distribution from various components in #1 gantry room and #2 fixed-beam room after 2-min treatment and 1-min cooling, whereas Fig. 4 shows that of 30-year continuous treatment and 1-min cooling. Detailed dose rate distributions at different conditions crossing the isocenter and along the BTL line in #1 gantry room and #2 fixed-beam room are shown in Fig. 5(a) and (b), respectively (the record line is along x-direction in Fig. 1, and are shown in the Figs. 3 (2) and (5)). Unless specified, the beam parameters are 230 MeV and 1.66 nA to patient point loss and 230 MeV and 0.106 nA to beam pipe line loss (Table 3).

It can be found from Figs. 3–5:

(1) After completion of the 2-min treatment (beam stopped hitting the patient), if the patient did not move, in the treatment room, the residual dose rate will be >2.5 μSv/h at a distance of <1 m at the cooling time of <10 min; the residual dose rate will reach 200 μSv/h at a distance of 30 cm at the cooling time of 1 min
(2) After a single short-time treatment, the residual dose rate declines quickly in the 30-min cooling time between two treatments: From 1 min to 5 min, it declines to approximately one-fourth; from 1 min to 10 min, declines to approximately 1/12; from 1 min to 30 min, it declines to approximately 1/55.
(3) After a single short-time treatment, the residual dose rate from the irradiated patient is almost the same from all components, especially close to the isocenter and in the 10-min cooling time, which indicates that the patient-induced radioactivity dominates the residual field in the treatment room in the 30-min treatment interval.
(4) After a single short-time treatment, the residual dose rate from the beam pipe is 1–3 orders of magnitude lower than that from all components, which indicates that the induced radioactivity results mainly from the source term of hitting patient; the other two source terms of beam loss from BTL to nozzle can be omitted as their annual workloads are 1–3 orders of magnitude lower than the former.
(5) After a single short-time treatment, at 1-min cooling, the residual dose rate from concrete, beam pipe, and nozzle, all <0.5 μSv/h in most space of the treatment room.
(6) In #2 fixed-beam room, after a single short-time treatment, at 1-min cooling, without couch, the concrete-produced residual dose rate at the corner downside of the beam direction will be >2.5 μSv/h. With couch (in our model), the concrete-produced dose rate at the corner will degrade to <1 μSv/h, and the couch-produced residual dose rate will reach approximately 5 μSv/h at the isocenter, as some secondary particles from hitting patient will be blocked by the couch.
(7) After 30-year continuous treatment, at 1-min cooling, the residual dose rate from concrete, beam pipe, and nozzle all will build up to 5–10 times, but still <2.5 μSv/h in most space of the treatment room. In #2 fixed-beam room, without couch, the concrete-produced residual dose rate at the corner downside of the beam direction may reach approximately 25 μSv/h. With couch, the residual dose rate from couch may reach approximately 80 μSv/h at the isocenter, both are comparable to the residual dose rate produced by patient after 2-min treatment. **However, the irradiation profile of 30-year continuous treatment is unreal and overestimated; in order to obtain the realistic result, we need to take the cooling process of each treatment into consideration. To do this, new formulas for calculating the activity buildup process of periodic irradiation were derived and extensively studied by the author, which are shown in Section 2.6.**
(8) By keeping the beam current fixed, and degrading the energy from 230 to 130 MeV, the residual dose rate will reduce 0.6 times of the former.
(9) The difference of residual dose distribution between gantry room and fixed-beam room is that the peak of isodose distributes along the lateral direction in the gantry room, but distributes along the forward direction in the fixed-beam room, due to their different beam directions at treating patient.

2.5. Air- and patient-induced radionuclides and dose rates from a single short-time treatment

As stated above, after a single short-time treatment, the residual dose rate is dominated by the patient, and the residual dose rate in the treatment room after 2-min treatment and 1-min

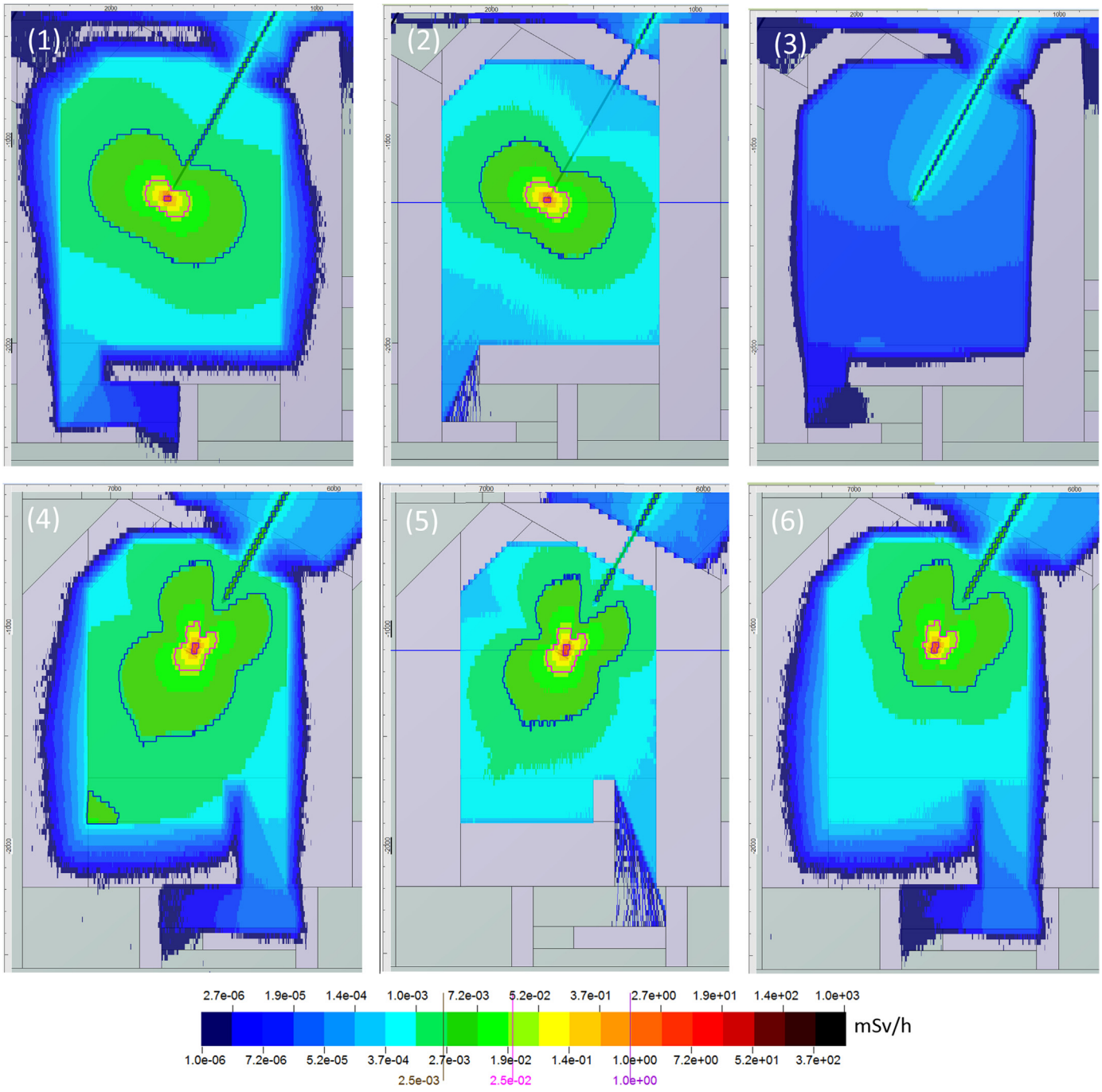

Fig. 3. Dose rate distribution in #1 gantry room and #2 fixed-beam room after 2-min treatment and 1-min cooling: (1) from all components in #1 gantry room; (2) from patient in #1 gantry room; (3) from beam pipe in #1 gantry room; (4) from all components in #2 fixed-beam room without couch; (5) from patient in #2 fixed-beam room without couch; (6) from all components in #2 fixed-beam room with couch.

cooling declines to half every 2 min in the 10-min cooling time. This indicates that the induced radioactivity dominates mainly by short-lived radionuclides with half-life about 2 min, which is produced by the patient. Table 5 shows air- and patient-produced main radionuclides, activity concentration, and dose rate at a distance of 1 m from the isocenter in the treatment room. In order to obtain Table 5, the air-inhaled effective dose coefficient and the air submersion dose coefficient were adopted from ICRP68 (Clement, 2012) and fgr12 (Eckerman and Ryman, 1993), respectively; the specific gamma-ray dose constant for radionuclides obtained from ORNL/RSIC-45 directly or calculated by the author using the method described in the same reference (Laurie and Trubey, 1982). In the calculation, except concrete, all the other components were assumed as linear source (for beam pipe) or point source (for patient, nozzle and couch), with 1/2 self-shielding factor, which was assumed by reviewing the mass–energy absorption coefficient, and the rationality is verified by the agreement of the total dose with FLUKA's simulation result (Fig. 5). To concrete, because it is not activated evenly and cannot be simplified as an ideal source, its total dose rate was adopted from FLUKA's simulation result and nuclide dose rate was obtained by multiplying the nuclide dose contribution to the total dose rate.

From Table 5, it can be found:

The induced radioactivity in the treatment room comes mainly from the patient after the single short-time treatment is completed. The main radionuclide is O-15, and its dose contribution

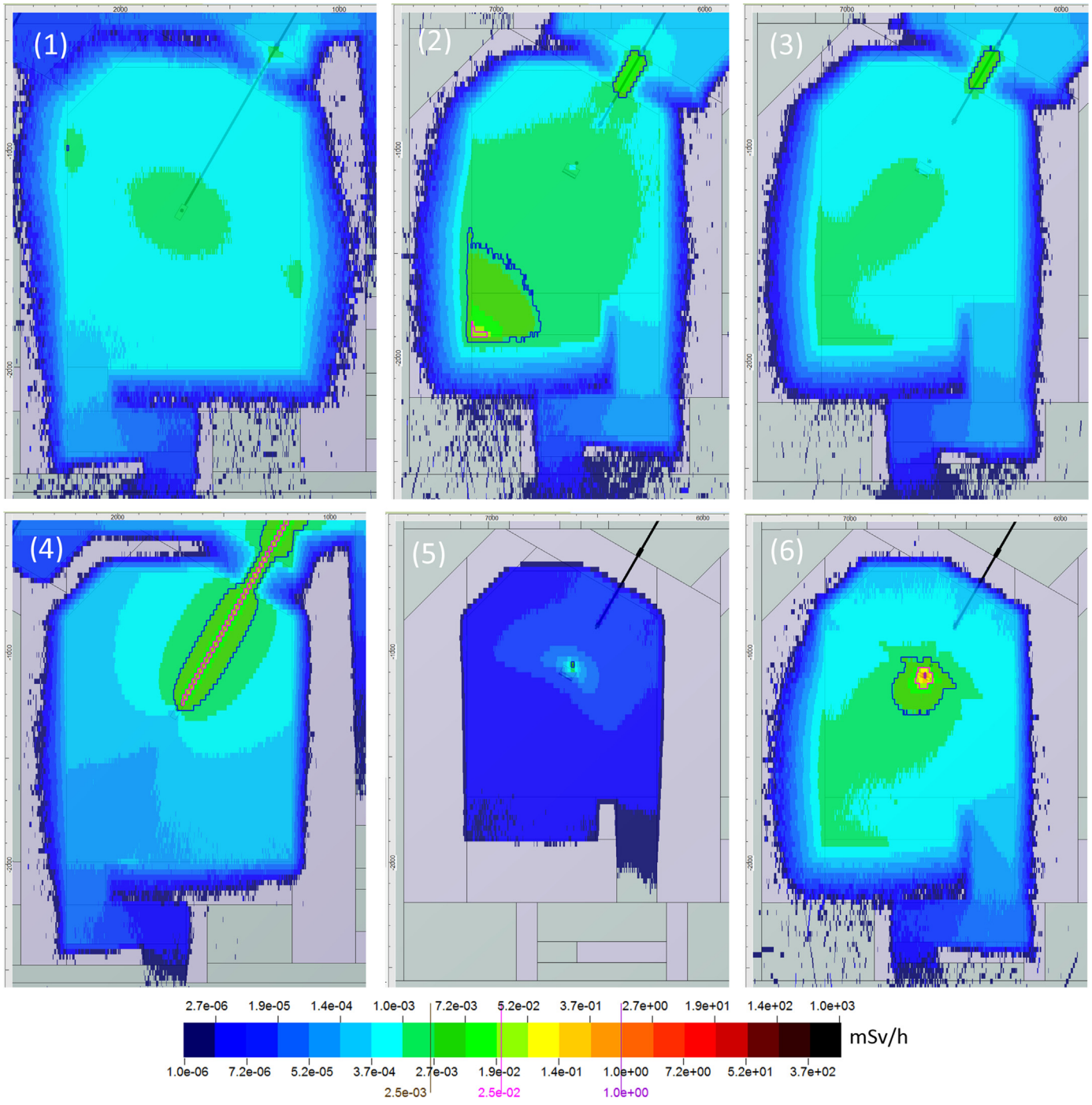

Fig. 4. Dose rate distribution from various components after 30-year continuous treatment and 1-min cooling: (1) from concrete in #1 gantry room: (2) from concrete in #2 fixed-beam room without couch; (3) from concrete in #2 fixed-beam room with couch; (4) from beam pipe in #1 gantry room: (5) from nozzle in #2 fixed-beam room with couch; (6) from couch in #2 fixed-beam room with couch.

accounts for 85% of all the patient's radionuclides. The O-15 is produced through $^{16}O(p, pn)\ ^{15}O$ reaction during treatment, while proton reaches the patient (water phantom). O-15 emits a pair of 0.511-MeV annihilation photons per decay by positron emission, then transforms into stable nuclide N-15.

(1) The activity concentration after 2-min treatment and 1-min cooling can be verified using activation formula, which are expressed in half-life by formulas (1) and (2) (Wu, 2014):

During irradiation (t_i is the irradiation time):

$$S(0 \le t \le t_i) = N\sigma\Phi\left(1 - 2^{-\frac{t}{T}}\right) \quad (1)$$

During cooling (t_c is the cooling time):

$$S(t = t_i + t_c) = N\sigma\Phi\left(1 - 2^{-\frac{t_i}{T}}\right)2^{-\frac{t_c}{T}} \quad (2)$$

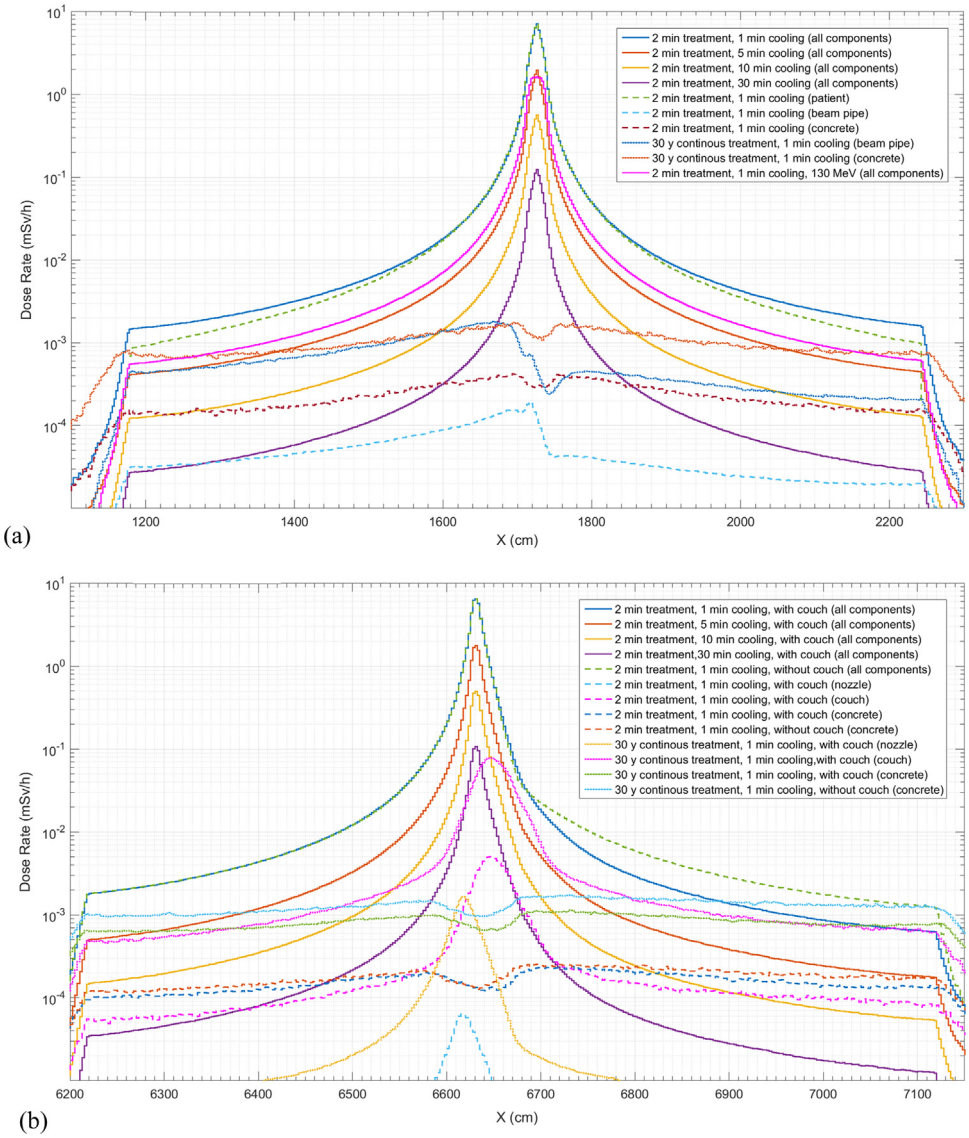

Fig. 5. (a) Dose rate distribution across the isocenter and along BTL at different cooling times in #1 gantry room at different conditions (components that produce the dose rates are shown in the parentheses). (b) Dose rate distribution across the isocenter and along BTL at different cooling times in #2 fixed-beam room at different conditions (components that produce the dose rates are shown in the parentheses).

where $N\left(cm^{-3}\right)$ is the atomic density of target material, $\Phi(cm^{-2}\bullet s^{-1})$ is the flux of the incident particle, σ is the production cross section of the radionuclide, $S_{sat}=N\sigma\Phi\left(\mathrm{Bq}\bullet cm^{-3}\right)$ is the saturation activity of the radionuclide for the continuous running, and T is the half-life of the radionuclide.

Take O-15 for example: The production cross section of various radionuclides in oxygen by proton bombardment can be found from Barbier (1969), as shown in Fig. 6, where it can be found that the reaction ^{16}O(p, pn) ^{15}O production cross section is 40–80 mb for proton energy between 20 and 230 MeV, and the average cross section can be taken as 60 mb. The thickness of the target (water phantom) is 30 cm, which is the range of proton in water with energy of 230 MeV, so the target can be assumed activated evenly. In the treatment room, the target (water phantom)'s cross-sectional area is A $=30\times 70$ cm, so the flux of incident proton with beam current I $=1.66$ nA is

$$\Phi=\frac{I}{A}=\frac{1.66\times10^{-9}\times6.25\times10^{18}}{30\times70}=4.94\times10^{6}(cm^{-2}\bullet s^{-1}),$$

where 6.25×10^{18} is the proton number for 1 coulomb electricity.

The atomic density of the target atom O-16 can be calculated using H_2O density ρ, molecule weight M, O-16 isotopic abundance θ, and Avogadro's constant N_A as

$$N=\frac{\rho}{M}\bullet N_A\bullet\theta=\frac{1}{18}\times6.02\times10^{23}\times0.99762=3.34\times10^{22}\left(cm^{-3}\right).$$

Substituting the average cross section σ=60mb and the other parameters into the activation formula (2), we obtain the activity concentration of O-15, after 2-min treatment with 230 MeV to 1.66 nA and 1-min cooling as

$$S=N\sigma\Phi\left(1-2^{-\frac{t_i}{T}}\right)2^{-\frac{t_c}{T_{1/2}}}=3.34\times10^{22}\times60\times10^{-3}\times10^{-24}\times4.94\times10^{6}\times\left(1-2^{-\frac{2\times60}{122}}\right)\times2^{-\frac{1\times60}{122}}=3.48\times10^{3}\left(\mathrm{Bq}\bullet cm^{-3}\right),$$

which agrees with FLUKA's simulation result in Table 5 completely.

(2) It is worth noting that there is H-3 and Be-7 (the two common isotopes in water activation) produced during patient's (water

Table 5
(a) Air- and patient-produced main radionuclides, activity concentration, and dose rate at a distance of 1 m from the isocenter in #1 gantry room, after 2-min treatment and 1-min cooling (nuclides with dose contribution < 1% not listed).

Component	A	Sym.	Z	Concentration (Bq/cm^3)	T (s)	Air-inhaled dose rate (mSv/h)	Air submersion dose rate (mSv/h)	Dose rate (mSv/h)	Nuclide's dose contribution (%)	Component's dose contribution (%)
Air	11	C	6	1.55E-04	1.22E+03	4.10E-07	2.55E-05	2.59E-05	14.91	0.69
	13	N	7	3.34E-04	5.98E+02	0.00E+00	5.49E-05	5.49E-05	31.60	
	15	O	8	5.63E-04	1.22E+02	0.00E+00	9.30E-05	9.30E-05	53.49	
	Total					4.10E-07	1.73E-04	1.74E-04	100.00	
Patient (water phantom)	10	C	6	2.54E+01	1.93E+01			2.54E-04	1.03	97.72
	11	C	6	1.70E+02	1.22E+03			1.02E-03	4.15	
	13	N	7	6.40E+01	5.98E+02			3.85E-04	1.56	
	14	O	8	1.27E+02	7.06E+01			1.89E-03	7.67	
	15	O	8	3.50E+03	1.22E+02			2.11E-02	85.58	
	Total							2.46E-02	100.00	

(b) Air- and patient-produced main radionuclides, activity concentration, and dose rate at a distance of 1 m from the isocenter in #2 fixed-beam room (with couch), after 2-min treatment and 1-min cooling (nuclides with dose contribution < 1% not listed).

Component	A	Sym.	Z	Concentration (Bq/cm^3)	T (s)	Air-inhaled dose rate (mSv/h)	Air submersion dose rate (mSv/h)	Dose rate (mSv/h)	Nuclide's dose contribution (%)	Component's dose contribution (%)
Air	11	C	6	2.62E-05	1.22E+03	6.91E-08	4.30E-06	4.37E-06	9.21	0.20
	13	N	7	1.03E-04	5.98E+02	0.00E+00	1.69E-05	1.69E-05	35.73	
	15	O	8	1.56E-04	1.22E+02	0.00E+00	2.58E-05	2.58E-05	54.31	
	Total					6.91E-08	4.74E-05	4.74E-05	100.00	
Patient (water phantom)	10	C	6	2.51E+01	1.93E+01			2.51E-04	1.06	97.41
	11	C	6	1.64E+02	1.22E+03			9.85E-04	4.17	
	13	N	7	6.05E+01	5.98E+02			3.64E-04	1.54	
	14	O	8	1.26E+02	7.06E+01			1.87E-03	7.92	
	15	O	8	3.35E+03	1.22E+02			2.02E-02	85.31	
	Total							2.36E-02	100.00	

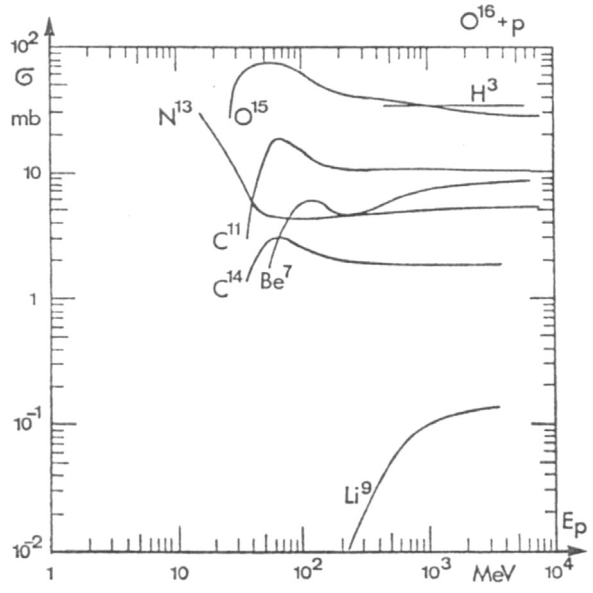

Fig. 6. Production cross section of various radionuclides in oxygen by proton bombardment from Barbier (1969).

phantom) activation process, but the 2-min treatment time is much shorter than the two isotopes' half-lives. The two isotopes are far from saturation (can be seen from the activation formula (1), where $t_i \ll T$), and their contribution to dose rate is far less than 1%, and hence both are not listed in Table 5.

(3) It can be seen from Table 5 that the air-inhaled dose rate is 3 orders of magnitude less than air submersion dose rate, sum of which is < 0.2 μSv/h, contributes only 0.7% to the total dose rate. Therefore, ventilation frequency of 1 time per hour does not result in air activation problem. We also calculated the nonradioactive toxic gases of O_3 and NO_2 produced by radiolysis in air, and found that it is not a problem either, because photon produced in proton accelerator is far less than that in electron accelerator. Thus, from both air activation and toxic gas production, it is unnecessary to change the ventilation frequently, to avoid the switch break down.

(4) Fig. 7 shows the decrease of residual dose rate with cooling time after 2-min treatment with 230 MeV and 1.66 nA. It can be seen that after 2-min treatment, the residual dose rate is dominated by the patient activation, in which O-15 dominates in the first 10 min of cooling, both O-15 and C-11 dominate in the cooling time between 10 and 15 min, and C-11 dominates after 15 min of cooling.

2.6. The components' radionuclides and dose rates from long-time treatment

2.6.1. Buildup formulas of periodic irradiation

For long-time treatment, excluding patient and air, the activity in other fixed components will build up. It is impossible to simulate the irradiation profile of HJPMF, as the treating and cooling cycles are too many to be written into FLUKA's input file. Therefore, in order to get the activity from long-time treatment, we simulated the 30-year continuous treating process (without beam cut-off time), but it is overestimated. Fortunately, the irradiation profile is periodic (although nested), the result from 30-year continuous treatment can be corrected by the formulas derived by the author, as presented below.

In the first day's treatment, the irradiation time for each treatment is $t_{i1}=2$ min, the cooling time is $t_{c1}=30$ min, the first-layer period is $t_1=t_{i1}+t_{c1}=32$ min. After $n_1=30$ cycles, the treatment time for each day is $t_{i2}=32$ min×30=16 h, the cooling time for each day is $t_{c2}=8$ h, the second-layer period is $t_2=t_{i2}+t_{c2}=24$ h=1 d. After $n_2=6$ cycles, the treatment time for each week is $t_{i3}=1$ d×6=6 days, the cooling time for each week is $t_{c3}=1$ d, the third-layer period is $t_3=t_{i3}+t_{c3}=1$ week. After $n_3=50$ cycles, the treatment time for each year is $t_{i4}=1$ week×50=50 weeks =350 days, the cooling time for each year

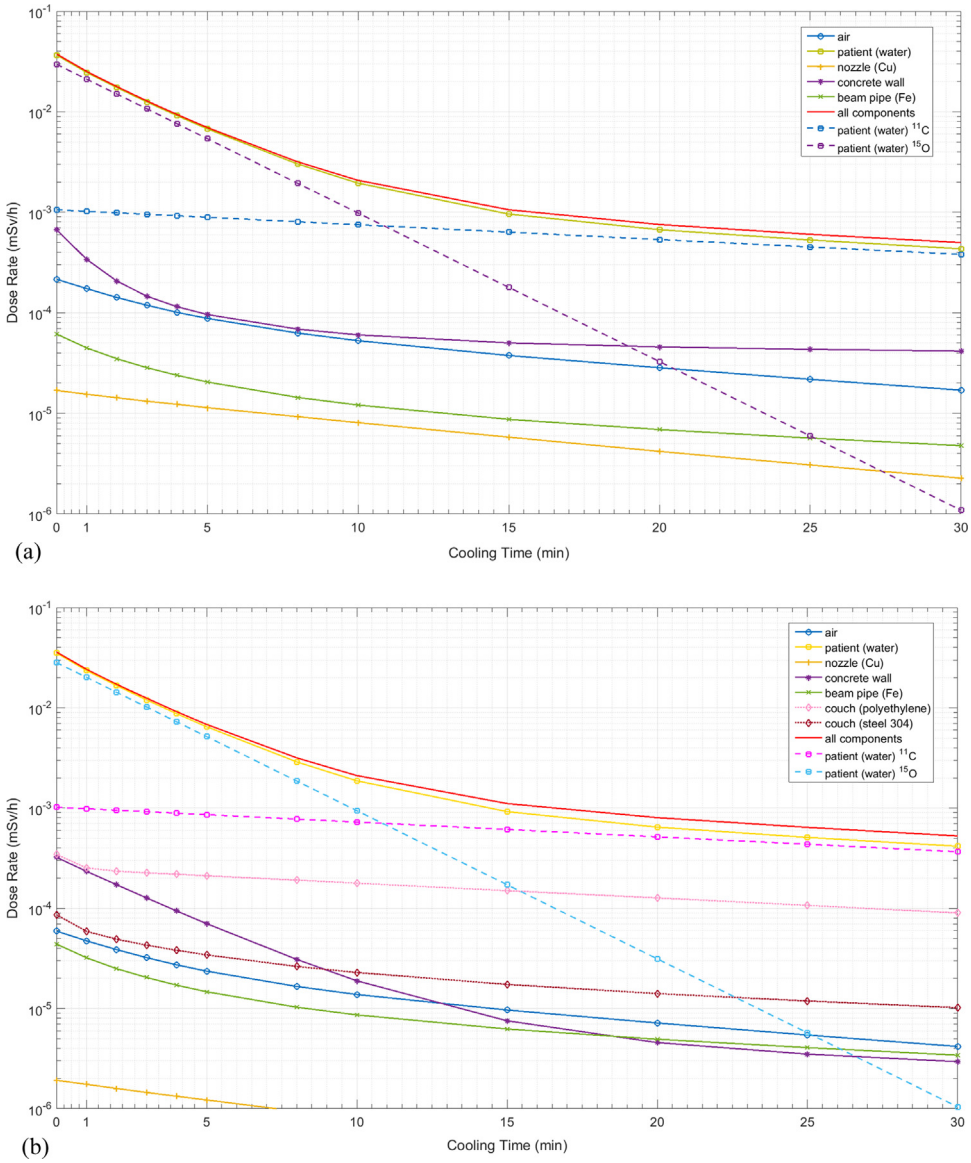

Fig. 7. (a) Decrease of dose rate with cooling time after 2-min treatment with 230 MeV and 1.66 nA, at a distance of 1 m from the isocenter in #1 gantry room, for different components and nuclides. (b) Decrease of dose rate with cooling time after 2-min treatment with 230 MeV and 1.66 nA, at a distance of 1 m from the isocenter in #2 fixed-beam room, for different components and nuclides.

is $t_{c4}=(365-350)$ days$=15$ days, the fourth-layer period is $t_4=1$ year $=365$ days. We assumed that the lifetime of HJPMF is 30 years, then $n_4=30$ cycles. From formulas (1) and (2), we obtain:

At the first irradiation-ending moment, the activity is

$$S_{i1} = N\sigma\Phi\left(1-2^{-t_{i1}/T}\right) = S_{sat}\left(1-2^{-t_{i1}/T}\right). \tag{3a}$$

At the first cooling-ending moment, the activity is

$$S_{c1} = S_{i1}\times 2^{-t_{c1}/T}. \tag{3b}$$

As each of the following treatments produces the same activity, after the first-layer n_1 cycle's treatment is completed, at the treatment-ending moment (the first day treatment-ending moment), the activity S_{i1} produced by each of the former treatments has cooled t_1, $2t_1$, … , $(n_1-1)t_1$, respectively, and the total activity been built up reaches a maximum value:

$$S_{1,max} = S_{i1}\times\left(1+2^{-\frac{t_1}{T}}+2^{-\frac{2t_1}{T}}+\ldots+2^{-\frac{(n_1-1)t_1}{T}}\right) = S_{i1}\times\left(\frac{1-2^{-\frac{n_1t_1}{T}}}{1-2^{-\frac{t_1}{T}}}\right). \tag{4a}$$

After the first-layer n_1 cycle treatment is completed, the cooling time extended from t_{c1} to $t_{c1}+t_{c2}$, the total activity been built up reaches a minimum value at the cooling-ending moment:

$$S_{1,min} = S_{1,max}\times 2^{-(t_{c1}+t_{c2})/T}. \tag{4b}$$

Similarly, after the second-layer n_2 cycle treatment is completed, at the treatment-ending moment (the first week treatment-ending moment), the activity $S_{1,max}$produced by each of former treatments has cooled t_2, $2t_2$, … , $(n_2-1)t_2$, respectively,

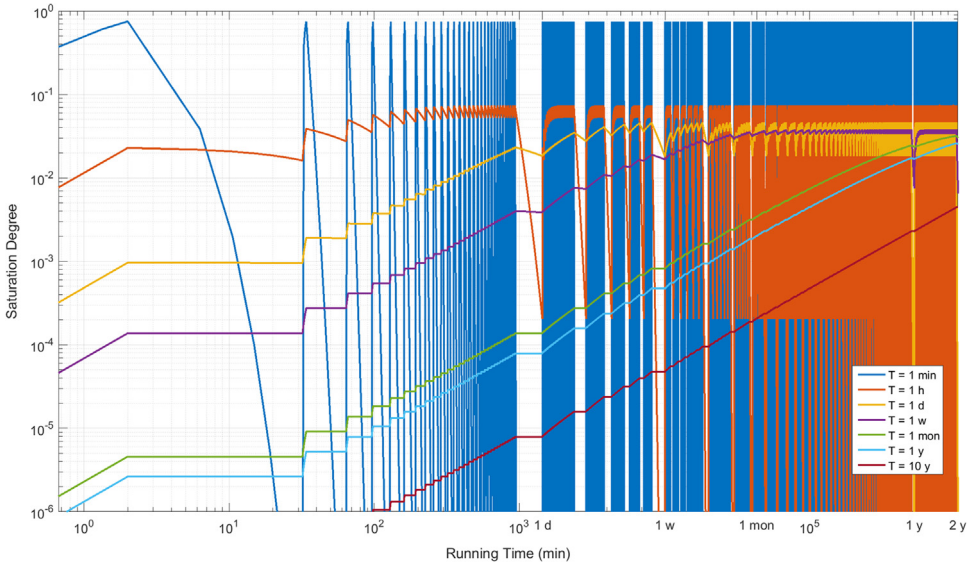

Fig. 8. Activity buildup process in the treatment room of HJPMF in 2 years for nuclides with different half-lives.

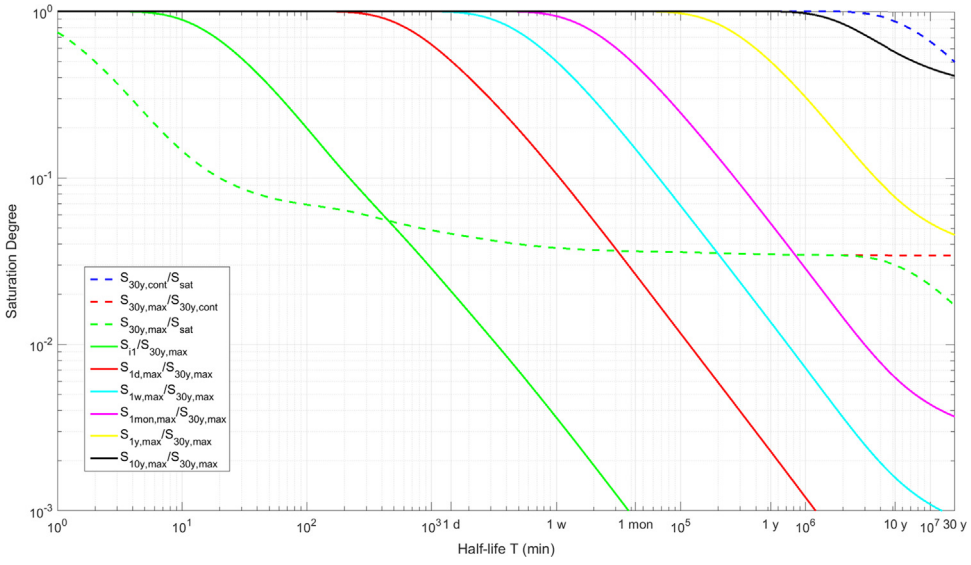

Fig. 9. Saturation degree as a function of nuclide half-life at different running time in HJPMF.

and the total activity been built up reaches a maximum value:

$$S_{2,max} = S_{1,max} \times \left(\frac{1-2^{-\frac{n_2 t_2}{T}}}{1-2^{-\frac{t_2}{T}}}\right) = S_{i1} \times \left(\frac{1-2^{-\frac{n_1 t_1}{T}}}{1-2^{-\frac{t_1}{T}}}\right) \times \left(\frac{1-2^{-\frac{n_2 t_2}{T}}}{1-2^{-\frac{t_2}{T}}}\right). \quad (5a)$$

After the second-layer n_2 cycle treatment is completed, the cooling time extended from t_{c1} to $t_{c1}+ t_{c2}+ t_{c3}$, the activity been built up reaches a minimum value at the cooling-ending moment:

$$S_{2,min} = S_{2,max} \times 2^{-(t_{c1}+t_{c2}+t_{c3})/T}. \quad (5b)$$

Similarly, after the kth-layer $n_k$cycle treatment is completed, the activity been built up reaches a maximum value and minimum value at the last treatment-ending moment and cooling-ending moment, respectively:

$$S_{k,max} = S_{k-1,max}\left(\frac{1-2^{-\frac{n_k t_k}{T}}}{1-2^{-\frac{t_k}{T}}}\right) = S_{i1}\prod_{l=1}^{k}\left(\frac{1-2^{-\frac{n_l t_l}{T}}}{1-2^{-\frac{t_l}{T}}}\right), \quad (6a)$$

$$S_{k,min} = S_{k,max} \times 2^{-\sum_{l=1}^{k+1} t_{cl}/T} = S_{i1} \times 2^{-\sum_{l=1}^{k+1} t_{cl}/T} \prod_{l=1}^{k}\left(\frac{1-2^{-\frac{n_l t_l}{T}}}{1-2^{-\frac{t_l}{T}}}\right), \quad (6b)$$

where l=1, 2,…,k,is the nested cycle layer and t_l, n_l, and $t_{cl}$are the period, cycle number, and cooling time of the lth cycle layer, respectively.

Eq. (6)a and b are new formulas for calculating the activity buildup process of periodic irradiation (nested or not), which are called as **buildup formulas of periodic irradiation**.

2.6.2. Activity buildup process and saturation degree

From the buildup formula (6a), we found two extreme cases:

Case 1:. The nuclide half-life is far less than each nested period ($T \ll t_l$). It means $2^{-\frac{t_l}{T}} \to 0$ and $2^{-\frac{n_l t_l}{T}} \to 0$. Formula (6a) can be simplified as $S_{k,max} = S_{i1} = S_{sat}\left(1-2^{-t_{i1}/T}\right)$, which indicates that **the maximum activity of the short-life nuclide is always the same as the first single treatment produced**, as it decays completely

Table 6

(a) Fixed components produced main radionuclides and dose rates at 1-min cooling at a distance of 1 m from the isocenter in #1 gantry room, after single 2-min treatment, 30-year continuous treatment, and 30-year periodic treatment. The saturation degree of 30-year periodic treatment is also listed (nuclides with dose contribution $<5\%$ not listed).

Component	Nuclide			Single 2-min treatment		Dose rate of 30-year continuous treatment (mSv/h)	Saturation degree ($S_{30y,max}/S_{30y,cont}$)	30-y periodic treatment		
	A	Sym.	T (s)	Dose rate (mSv/h)	Contribution (%)			Concentration (Bq/cm^3)	Dose rate (mSv/h)	Contribution (%)
	61	Cu	1.20E+04	1.89E-07	1.25	2.73E-05	6.39E-02	1.09E+01	1.75E-06	7.70
	62	Cu	5.84E+02	1.36E-05	90.59	1.03E-04	1.48E-01	7.66E+01	1.52E-05	67.03
	64	Cu	4.57E+04	5.48E-08	0.36	3.01E-05	5.05E-02	4.11E+01	1.52E-06	6.72
	Total			1.51E-05	100.00	2.45E-04		1.84E+02	2.27E-05	100.00
Concrete wall	15	O	1.22E+02	4.79E-05	21.46	9.70E-05	4.94E-01	6.58E-03	4.79E-05	18.05
	24	Na	5.39E+04	1.23E-06	0.55	7.98E-04	4.93E-02	2.02E-03	3.93E-05	14.82
	28	Al	1.35E+02	1.66E-04	74.54	3.61E-04	4.61E-01	1.85E-02	1.66E-04	62.68
	Total			2.23E-04	100.00	1.39E-03		2.98E-02	2.65E-04	100.00
Beam pipe (Fe)	48	V	1.38E+06	7.95E-09	0.02	1.32E-04	3.67E-02	5.97E+00	4.84E-06	6.54
	52	Mn	4.83E+05	3.09E-08	0.07	1.80E-04	3.85E-02	7.21E+00	6.92E-06	9.33
	53	Fe	5.11E+02	8.62E-06	19.91	5.73E-05	1.62E-01	2.38E+01	9.30E-06	12.56
	54	Mn	2.70E+07	3.65E-10	0.00	1.18E-04	3.48E-02	1.68E+01	4.12E-06	5.56
	52 m	Mn	1.27E+03	6.91E-06	15.97	1.09E-04	9.78E-02	1.55E+01	1.06E-05	14.34
	52 m	Fe	4.59E+01	4.71E-06	10.89	5.63E-06	8.37E-01	3.46E+00	4.71E-06	6.36
	53 m	Fe	1.55E+02	2.01E-05	46.40	4.83E-05	4.16E-01	2.43E+01	2.01E-05	27.11
	Total			4.33E-05	100.00	8.91E-04		1.95E+02	7.41E-05	100.00
Total of all components				2.51E-02		2.73E-02			2.51E-02	
Total after moving out of patient				4.55E-04		2.70E-03			5.36E-04	

(b) Fixed components produced main radionuclides, dose rates at a distance of 1 m from the isocenter in #2 fixed-beam room (with couch), after 2-min single short-time treatment or 30-year periodic treatment (nuclides with dose contribution $<5\%$ not listed).

Component	Nuclide			Single 2-min treatment			30-year periodic treatment					
	A	Sym.	T (s)	Dose rate at 1-min cooling (mSv/h)	Nuclide's dose contribution (%)	Component's dose contribution (%)	Dose rate at 1-min cooling (mSv/h)	Nuclide's dose contribution (%)	Component's dose contribution (%)	Dose rate at 10-min cooling (mSv/h)	Nuclide's dose contribution (%)	Component's dose contribution (%)
Nozzle (Cu)	62	Cu	5.84E+02	1.09E-06	62.72	0.01	1.21E-06	35.04	0.01	6.39E-07	26.05	0.11
	64	Cu	4.57E+04	5.51E-08	3.18		1.53E-06	44.31		1.52E-06	61.99	
	66	Cu	3.05E+02	5.85E-07	33.76		5.93E-07	17.15		1.74E-07	7.10	
				1.73E-06	100.00		3.46E-06	100.00		2.45E-06	100.00	
	Total											
Concrete wall	11	C	1.22E+03	2.50E-06	1.46	0.71	3.77E-06	1.86	0.83	2.77E-06	6.15	1.94
	15	O	1.22E+02	4.08E-05	23.90		4.08E-05	20.15		1.91E-06	4.24	
	24	Na	5.39E+04	9.09E-07	0.53		2.90E-05	14.32		2.88E-05	63.95	
	28	Al	1.35E+02	1.21E-04	70.85		1.21E-04	59.75		7.49E-06	16.62	
				1.71E-04	100.00		2.03E-04	100.00		4.51E-05	100.00	
	Total											
Beam pipe (Fe)	48	V	1.38E+06	5.66E-09	0.02	0.13	3.45E-06	6.50	0.22	3.45E-06	10.82	1.37
	52	Mn	4.83E+05	2.21E-08	0.07		4.95E-06	9.32		4.95E-06	15.51	
	53	Fe	5.11E+02	6.18E-06	19.92		6.67E-06	12.56		4.74E-06	14.85	
	54	Mn	2.70E+07	2.63E-10	0.00		2.97E-06	5.59		2.97E-06	9.30	
	56	Co	6.68E+06	7.68E-10	0.00		2.20E-06	4.14		2.20E-06	6.90	
	52 m	Mn	1.27E+03	4.95E-06	15.96		7.61E-06	14.33		5.66E-06	17.75	
	52 m	Fe	4.59E+01	3.37E-06	10.87		3.37E-06	6.35		9.69E-10	0.00	
	53 m	Fe	1.55E+02	1.44E-05	46.43		1.44E-05	27.13		1.28E-06	4.02	
				3.10E-05	100.00		5.31E-05	100.00		3.19E-05	100.00	
	Total											
Couch	11	C	1.22E+03	2.41E-04	95.34	1.05	3.64E-04	96.32	1.55	2.68E-04	99.06	11.63

Table 6 (*continued*)

(b) Fixed components produced main radionuclides, dose rates at a distance of 1 m from the isocenter in #2 fixed-beam room (with couch), after 2-min single short-time treatment or 30-year periodic treatment (nuclides with dose contribution < 5% not listed).

Component	Nuclide			Single 2-min treatment			30-year periodic treatment				
	A	Sym.	T (s)	Dose rate at 1-min cooling (mSv/h)	Nuclide's dose contribution (%)	Component's dose contribution (%)	Dose rate at 1-min cooling (mSv/h)	Nuclide's dose contribution (%)	Component's dose contribution (%)	Dose rate at 10-min cooling (mSv/h)	Nuclide's dose contribution (%)	Component's dose contribution (%)
(polyethylene)				2.53E-04	100.00		3.78E-04	100.00		2.71E-04	100.00	
	Total											
Couch (steel 304)	28	Al	1.35E+02	3.15E-06	5.26	0.25	3.15E-06	2.40	0.54	1.95E-07	0.21	3.92
	48	V	1.38E+06	1.35E-08	0.02		8.23E-06	6.26		8.23E-06	9.02	
	52	V	2.25E+02	1.07E-05	17.81		1.07E-05	8.14		2.03E-06	2.22	
	52	Mn	4.83E+05	3.59E-08	0.06		8.03E-06	6.11		8.03E-06	8.80	
	53	Fe	5.11E+02	9.70E-06	16.20		1.05E-05	7.97		7.44E-06	8.16	
	54	Mn	2.70E+07	1.20E-09	0.00		1.36E-05	10.33		1.36E-05	14.89	
	56	Mn	9.28E+03	2.43E-06	4.06		1.80E-05	13.70		1.73E-05	18.96	
	56	Co	6.68E+06	1.96E-09	0.00		5.62E-06	4.27		5.62E-06	6.16	
	52 m	Mn	1.27E+03	8.34E-06	13.92		1.28E-05	9.76		9.54E-06	10.46	
	53 m	Fe	1.55E+02	2.26E-05	37.82		2.26E-05	17.24		2.02E-06	2.21	
				5.99E-05	100.00		1.31E-04	100.00		9.12E-05	100.00	
	Total											
Total of all components				2.42E-02		100.00	2.44E-02		100.00	2.33E-03		100.00
Total after moving out of patient				5.64E-04		2.33	8.16E-04		3.34	4.55E-04		19.56

before the next treatment starts. Furthermore, if $T \ll t_{i1}$ is also satisfied, the nuclide can reach its ideal saturation at any treatment-ending moment. This case is shown in Fig. 8 by the curve "T = 1 min"

Case 2:. The nuclide half-life is far longer than each nested period ($T \gg t_l$). It means $\frac{t_l}{T} \to 0$ and $\frac{n_l t_l}{T} \to 0$. Using the limitation of $2^{-x} = 1+\frac{-1\times \ln 2}{1!}x+\cdots = 1-(\ln 2)x(x \to 0)$, formula (6a) can be simplified as.

$$S_{k,\max} = S_{i1}\prod_{l=1}^{k}\left(\frac{1-2^{-\frac{n_l t_l}{T}}}{1-2^{\frac{t_l}{T}}}\right) = S_{i1}\prod_{l=1}^{k} n_l, \tag{7a}$$

where, $\prod_{l=1}^{k} n_l$ is the total number of treatment and $S_{i1}$is the activity produced by a single treatment.

Formula (7a) shows that **for the long-life nuclide, its cooling process could be neglected, its activity increases proportionally with total number of treatment**. This case is shown in Fig. 8 by the curve "T = 10 y."

Substituting formula (3a) into formula (7a), we obtain

$$\begin{aligned} S_{k,max} &= S_{sat}\left(1-2^{-t_{i1}/T}\right)\prod_{l=1}^{k} n_l = S_{sat}\left((\ln 2)\frac{t_{i1}}{T}\right)\prod_{l=1}^{k} n_l \\ &= S_{sat}\left((\ln 2)\frac{\left(\prod_{l=1}^{k} n_l\right)t_{i1}}{T}\right)\frac{t_{tot}}{t_{tot}} = S_{sat}\left((\ln 2)\frac{t_{tot}}{T}\right)\frac{\left(\prod_{l=1}^{k} n_l\right)t_{i1}}{t_{tot}} \\ &= S_{sat}\left(1-2^{-\frac{t_{tot}}{T}}\right)\frac{\left(\prod_{l=1}^{k} n_l\right)t_{i1}}{t_{tot}} = S_{sat}\frac{t_{itot}}{t_{tot}}\left(1-2^{-\frac{t_{tot}}{T}}\right) \\ &= N\sigma\left(\Phi\frac{t_{itot}}{t_{tot}}\right)\left(1-2^{-\frac{t_{tot}}{T}}\right), \end{aligned} \tag{7b}$$

where, $t_{tot} \ll T$ is the total time starting from the first treatment, $t_{itot} = \left(\prod_{l=1}^{k} n_l\right)t_{i1}$ is the corresponding total irradiation time, and $\frac{t_{itot}}{t_{tot}}$ is the duty factor of irradiation time.

Formula (7b) shows that **for the long-life nuclide, its activity could be calculated as continuous irradiation, but the beam current (or flux) must be decreased by multiplying the duty factor of irradiation tim**e. Accordingly, for the periodic irradiation, saturation activity of the long-life nuclide is no longer its ideal saturation S_{sat}, but $S_{sat}\frac{t_{itot}}{t_{tot}}$. The duty factor of HJPMF for irradiation time of 30 years is

$$\frac{t_{itot}}{t_{tot}} = \frac{\left(\prod_{l=1}^{4} n_l\right)t_{i1}}{30y} = \frac{30\times 6\times 50\times 30\times 2min}{30y} = \frac{300h}{1y} = 0.034.$$

Therefore, the saturation activity of the long half-life nuclide is only 0.034 times of its ideal saturation.

The direct way of finding the activity build-up process is adding up the activity produced by each of the former irradiation. To HJPMF, it is programmed and shown in Fig. 8.

It is very important to determine theoretically what saturation degree of each nuclide can reach during the accelerator's life-time, and how fast it does. For this purpose, formula (6a) can be used to define and calculate the saturation degree at different running times, typically 30-year saturation degree $\left(\frac{S_{30y,cont}}{S_{sat}}, \frac{S_{30y,max}}{S_{30y,cont}} \text{or} \frac{S_{30y,max}}{S_{sat}}\right)$, single-treatment saturation degree $\left(\frac{S_{i1}}{S_{30y,max}}\right)$, 1-day saturation degree $\left(\frac{S_{1d,max}}{S_{30y,max}}\right)$, 1-week saturation degree $\left(\frac{S_{1w,max}}{S_{30y,max}}\right)$, 1-month saturation degree $\left(\frac{S_{1mon,max}}{S_{30y,max}}\right)$, 1-year saturation degree $\left(\frac{S_{1y,max}}{S_{30y,max}}\right)$, 10-year saturation degree $\left(\frac{S_{10y,max}}{S_{30y,max}}\right)$, and so on, where, $S_{30y,cont}$ is the activity at

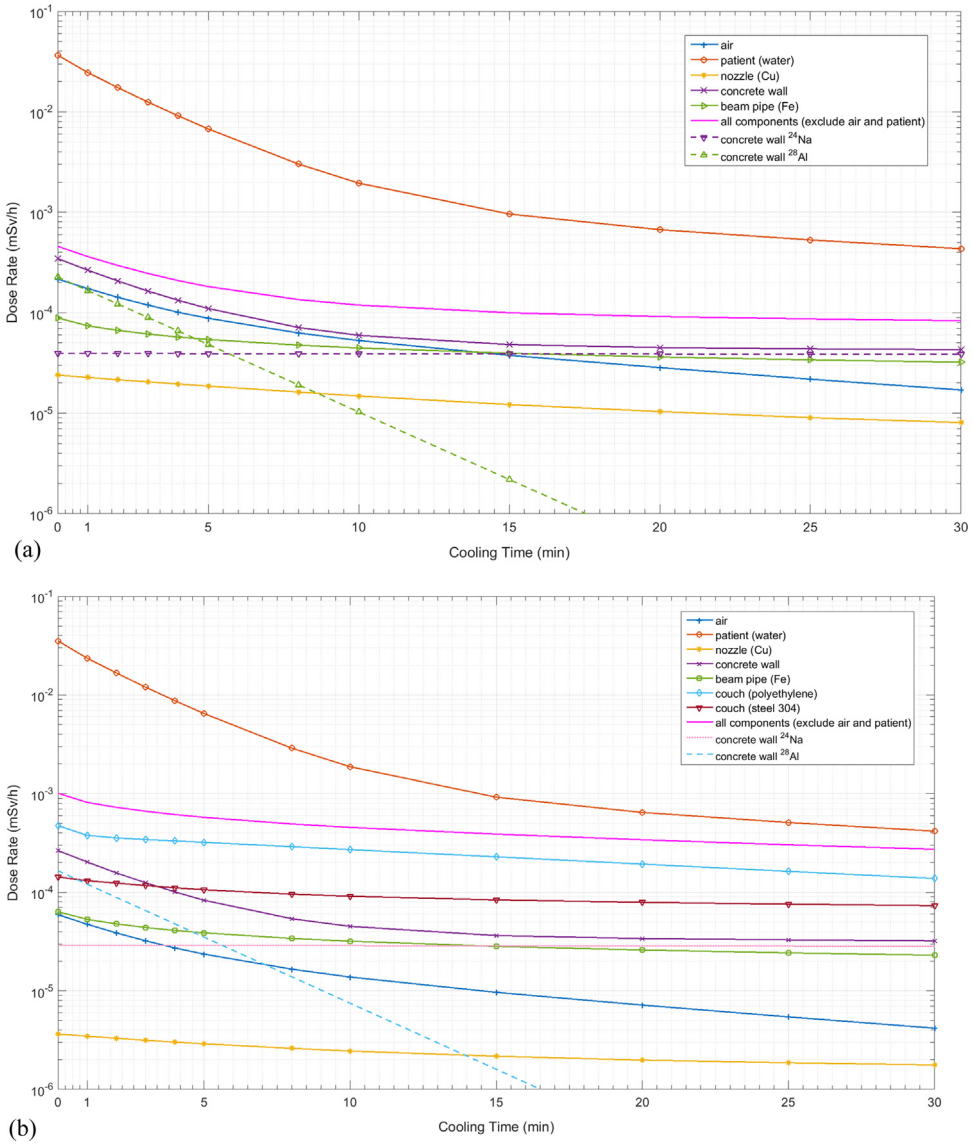

Fig. 10. (a) Decrease of dose rate with cooling time, after 30-y periodic treatment with 230 MeV and 1.66 nA, at a distance of 1 m from the isocenter in #1 gantry room, for different components and nuclides. (b) Decrease of dose rate with cooling time, after 30-y periodic treatment with 230 MeV and 1.66 nA, at a distance of 1 m from the isocenter in #2 fixed-beam room, for different components and nuclides.

30-year continuous treatment-ending moment; $S_{1d,max}$, $S_{1w,max}$, $S_{1mon,max}$, $S_{1y,max}$, and $S_{10y,max}$ are the saturation at the treatment-ending moment of 1d, 1 week, 1 month, 1 year, and 10 years, respectively. All these quantities are functions of the nuclide half-life, as plotted in Fig. 9.

From Fig. 9, it can be found that: **With the increase of half-life, the nuclide not only needs longer time to reach saturation, but also decreases its saturation degree**. Nuclides with half-life <5 min could reach saturation in a single treatment, their 30-year saturation degree ranges from 1 to 0.24. Nuclides with half-life ranging from 5 min to 4 h could reach saturation in 1 day, and their saturation degree ranges from 0.24 to 0.062. Nuclides with half-life ranging from 4 h to 1 day could reach saturation in 1 week, and their saturation degree ranges from 0.062 to 0.046. Nuclides with half-life ranging from 1d to 1 week could reach saturation in 1 month, and their saturation degree ranges from 0.046 to 0.038. Nuclides with half-life ranging from 1 week to 2 months could reach saturation in 1 year, their saturation degree ranges from 0.038 to 0.036. Nuclides with half-life ranging from 2 months to 2 years could reach saturation in 10 years, and their saturation degree ranges from 0.036 to 0.035. Nuclides with half-life ranging from 2 to 6 years could reach saturation in 30 years, their saturation degree ranges from 0.035 to 0.034. Nuclides with half-life >6 years could not reach ideal saturation in the 30-year lifetime, and their 30-year saturation degree $\frac{S_{30y,max}}{S_{sat}}$ ranges from 0.034 to 0.017, but $\frac{S_{30y,max}}{S_{30y,cont}}$ keeps at 0.034.

Formula (6a) and Fig. 9 are important to find the activity buildup process of a known nuclide. For example, ^{24}Na (produced by ^{23}Na(n,γ)^{24}Na reaction) is commonly found in concrete and its half-life is 15 h. It is evident from Fig. 9 that the single-treatment saturation degree $\left(\frac{S_{i1}}{S_{30y,max}}\right)$ is 0.03, which indicates that its single-treatment activity will build up 33 times once it reaches saturation; furthermore, its 1-week saturation degree $\left(\frac{S_{1w,max}}{S_{30y,max}}\right)$ is 1, which shows that it could reach saturation in the first week; its 30-year saturation degree $\left(\frac{S_{30y,max}}{S_{sat}}\right)$ is 0.05, which indicates that its activity is only 1/20 of the ideal saturation when it reaches saturation, which equivalently decreases its production cross section

Table 7
Dose rate and integral dose received by the patient escort from patient-induced radioactivity at different contact distance and cooling time, after a single 2-min treatment with 230 MeV and 1.66 nA.

Distance to irradiated patient	Cooling time	Maximal dose rate (mSv/h)	Minimal dose rate (mSv/h)	Maximal integral dose (mSv)	Minimal integral dose (mSv)	Average integral dose (mSv)
30 cm	1–5 min	2.73E-01	7.46E-02	1.82E-02	4.97E-03	9.52E-03
	5–10 min	7.46E-02	2.15E-02	6.21E-03	1.79E-03	3.33E-03
	10–30 min	2.15E-02	4.75E-03	7.15E-03	1.58E-03	3.36E-03
	30 min–1 h	4.75E-03	1.57E-03	2.37E-03	7.87E-04	1.37E-03
	1–4 h	1.57E-03	4.20E-06	4.72E-03	1.26E-05	2.44E-04
	4 h–1day	4.20E-06	1.61E-07	8.40E-05	3.22E-06	1.64E-05
	1 d–1 week	1.61E-07	5.45E-08	2.32E-05	7.85E-06	1.35E-05
	1 week–1 year	5.45E-08	1.00E-08	4.68E-04	8.59E-05	2.01E-04
60 cm	1–5 min	7.28E-02	1.99E-02	4.86E-03	1.33E-03	2.54E-03
	5–10 min	1.99E-02	5.73E-03	1.66E-03	4.77E-04	8.89E-04
	10–30 min	5.73E-03	1.27E-03	1.91E-03	4.23E-04	8.98E-04
	30 min–1 h	1.27E-03	4.20E-04	6.34E-04	2.10E-04	3.65E-04
	1–4 h	4.20E-04	1.33E-06	1.26E-03	3.99E-06	7.09E-05
	4 h–1 d	1.33E-06	8.92E-08	2.66E-05	1.78E-06	6.89E-06
	1 d–1 week	8.92E-08	1.61E-08	1.28E-05	2.32E-06	5.46E-06
	1 week–1 year	1.61E-08	1.00E-09	1.38E-04	8.59E-06	3.45E-05
1 m	1–5 min	2.69E-02	7.36E-03	1.80E-03	4.91E-04	9.39E-04
	5–10 min	7.36E-03	2.12E-03	6.13E-04	1.77E-04	3.30E-04
	10–30 min	2.12E-03	4.70E-04	7.08E-04	1.57E-04	3.33E-04
	30 min–1 h	4.70E-04	1.55E-04	2.35E-04	7.77E-05	1.35E-04
	1–4 h	1.55E-04	6.05E-07	4.66E-04	1.82E-06	2.91E-05
	4 h–1 d	6.05E-07	6.25E-08	1.21E-05	1.25E-06	3.89E-06
	1day–1 week	6.25E-08	6.59E-09	9.00E-06	9.49E-07	2.92E-06
	1 week–1 year	6.59E-09	6.00E-11	5.66E-05	5.16E-07	5.40E-06

to 1/20 of its original as compared to those short-lifetime nuclide, which can almost reach ideal saturation by a single short-time treatment.

2.6.3. Fixed components' radionuclides and dose rates from long-time treatment

Table 6 shows the fixed components' main radionuclides, dose rate at a distance of 1 m from isocenter in #1 gantry room and #2 fixed-beam room (with couch), after 2-min short-time treatment or 30-year periodic treatment. Fig. 10 shows the decrease of dose rate with cooling time, after 30-year treatment with 230 MeV and 1.66 nA, at 1 m from isocenter in #2 fixed-beam room (the patient is assumed without movement), for different components and nuclides. It can be found from Table 6 and Fig. 10:

(1) To the fixed components, their dose rate at 1-min cooling from 30-year periodic treatment are at most 2.2 times of that of 2 min single short-time treatment, lower than ever expected, because the saturation degree of middle- and long- lifetime nuclide decreases obviously by long cooling time and short treating time, as previously stated.
(2) Even after long-time treatment, the residual dose rate at a distance of 1 m from the isocenter is still dominated by the patient in the cooling time of 30 min, but the patient's dose contribution decreases quickly with time, from approximately 97% (at 1-min cooling) to 70% (at 15-min cooling), until 60% (at 30-min cooling), because the main nuclides produced in patient are still the two short-lifetime nuclides, O-15 and C-11, but more middle- and long- lifetime nuclides are built up in other fixed components.
(3) The second contributor to dose rate is concrete wall or couch, which depends on the couch's structure, material, thickness, and placement. Both of them contribute 0.2–0.5 μSv/h at 1-min cooling at a distance of 1 m from the isocenter.
(4) In our simulation, the couch's main material is polyethylene, and its main radionuclide is C-11, which is produced by the fast neutron reaction $^{12}C(n,2n)^{11}C$, and the fast neutron comes mainly from the $^{16}O(p,pn)^{15}O$ in the patient. This nuclide contributes approximately 0.4 μSv/h at 1-min cooling.
(5) In Section 2.4, we found that the dose rate at 1-min cooling from couch at the isocenter will be approximately 5 μSv/h after a single short-time treatment, and will build up to approximately 80 μSv/h after 30-year continuous treatment. However, by adopting the buildup formulas to correct, after 30-years periodic treatment, it will build up to approximately 8 μSv/h, which is one-tenth of that after 30-year continuous treatment, and is still much less than the dose rate from patient.
(6) In our simulation, the concrete material adopted from FLUKA manual (Ferrari et al., 2011), the author once compared the element composition from several references (Wu, 2014), and found that there is no significant difference, except the concrete from J-PARC without sodium (Tokai-mura and Ibaraki-ken, 2004). From Table 6, Al-28 and Na-24 are the two main radionuclides produced in concrete after long-time treatment and in the 30-min cooling time. Al-28 is the short-lifetime nuclide, and Na-24 is the middle-lifetime nuclide, and hence the former dominates the dose rate produced by concrete in the cooling time of 0–5 min and the later dominates the dose rate produced by concrete in the cooling time of 5–30 min. By simulation, we found that the activity of

Table 8
The patient escort received integral dose at different contact distance and begin contact time.

Average contact distance to irradiated patient	Begin contact time after treatment finished (min)	Integral dose received by the escort from each treatment (mSv)	Average absorbed dose for the patient been cured (Gy)	Average absorbed dose of the patient in each treatment (Gy)	Number of treatments for the patient been cured	Integral dose received by the escort from the patient been cured (mSv)
30 cm	1	1.81E-02	70	2.72	25.71	4.64E-01
	5	8.54E-03				2.20E-01
60 cm	1	4.81E-03				1.24E-01
	5	2.27E-03				5.84E-02
1 m	1	1.78E-03				4.57E-02
	5	8.39E-04				2.16E-02

Table 9
Dose received by the positioning technician from removing the irradiated patient from couch (1 min assumed to contact the irradiated patient).

Average contact distance to irradiated patient	Begin contact time after treatment finished (min)	Integral dose from each remove (mSv)	Number of patients removed per day per room	Total number of patients removed per year	All room's annual dose from removing the irradiated patient (mSv/a)	Number of positioning technicians (assumed)	Annual dose received by each positioning technician (mSv/a)
60 cm	1	1.21E-03			5.46E+01		1.09E+01
	5	3.31E-04			1.49E+01		2.98E+00
	10	9.55E-05	30	45,000	4.30E+00	5	8.59E-01
1 m	1	4.49E-04			2.02E+01		4.04E+00
	5	1.23E-04			5.52E+00		1.10E+00
	10	3.54E-05			1.59E+00		3.19E-01

Table 10
Dose received by the positioning technician from positioning the next patient (10 min assumed in the process of position, dose rate adopted that of #2 fixed-beam room with couch.).

Average distance to isocenter	Dose rate at 1-min cooling at saturation state from fixed components (mSv/h)	Integral dose from each position (mSv)	Number of patients positioned per day per room	Total number of patients positioned per year	All room's annual dose from position (mSv/a)	Number of positioning technicians (assumed)	Annual dose received by each positioning technician (mSv/a)
1 m	8.16E-04	1.01E-04	30	45,000	4.55	5	0.91

Na-24 produced by concrete without sodium decreases to approximately 1/17 of concrete with sodium.

(7) Only two dominating nuclides, Cu-62 and Cu-64, are produced in nozzle (Cu), whereas many main nuclides are produced in beam pipe, including Mn-52, Fe-53, Mn-52 m, and Fe-53 m.

2.7. Radiation protection for the patient escort

In order to evaluate the radiation influence of patient-induced activity to his/her surrounding environment, we calculated the residual dose rate produced by the patient at different distances and cooling times, and the integral dose at these cooling time intervals, as shown in Table 7. It is evident from the table that the maximal integral dose (column #5) and minimal integral dose (column #6) result from the cooling time interval (column #2) multiplied by the maximal dose rate (column #3) and minimal dose rate (column #4), respectively; the average integral dose (the last column) result from the geometric mean of the maximal integral dose (column #5) and the minimal integral dose (column #6).

For simple and conservative calculation, we assumed the patient could be cured in 1 year, the escort began to contact the patient at 1 or 5 min after the treatment is completed, the average contact distance is 30 cm, 60 cm, or 1 m. Then, the escort's annual dose from the patient's activation can be calculated by multiplying the number of treatments for the patient been cured to the integral dose from each treatment, as shown in Table 8. It is evident from the table that the integral dose received by the escort from each treatment (column #3) results from the summation of average integral dose of cooling time of 1 min to 1 year in Table 7. The average absorbed dose needed for the patient been cured (column #4) comes from IBA's treatment assumption (Stichelbaut, 2014b); the number of treatments for the patient been cured (column #6) comes from total treatment number (30 patients per day multiplied by 300 days per year), divided by the total patients (350 per room per year) (Stichelbaut, 2014b); the average absorbed dose of the patient in each treatment (column #5) comes from the total absorbed dose (column #4) divided by the total number of treatments (column #6). From Table 8, we found that the annual dose received by the escort is 0.464 mSv/a, at the contact distance and cooling time of 30 cm and 1 min, respectively. In practice, the begin contact time maybe 5 min after the treatment finished or later, and the average contact distance maybe 60 cm or farther. In that case, the annual dose received by the escort obtained from patient-induced radioactivity will be at most 0.058 mSv/a, less than HJPMF's govern target value (0.1 mSv/a) for the public.

2.8. Radiation protection for the positioning technician

After a treatment is completed, the positioning technician needs to enter the treatment room to remove the irradiated patient from couch and position the next patient. In this process, the main radiation source, that is, the patient, together with other components, will induce some radiation to the positioning technician.

2.8.1. Dose received from removing the irradiated patient

The annual dose received by the positioning technician from removing the irradiated patient can be calculated by multiplying the total number of removal and the integral dose from each removal. According to the annual workload data presented in Table 2, we assumed the following: each treatment room allocated one positioning technician, the average contact time needed to remove the patient from couch is 1 min, the average contact distance was 60 cm or 1 m, and the begin contact time after completion of treatment was 1, 5, or 10 min. Then, the dose received by the positioning technician from removing the irradiated patient can be calculated as shown in Table 9.

From Table 9, the positioning technician will receive an annual dose of 4 mSv/a from removing the irradiated patient at the average contact distance of 1 m and begin contact time of 1 min; this annual dose can be decreased to 1.1 mSv/a or even 0.319 mSv/a if the begin contact time postpones to 5 or 10 min after treatment is complete. Longer wait is unnecessary and unrealistic:

Unnecessary – After 10-min cooling, the residual dose rate at 1 m (dominated by patient) has decayed to 2.33 μSv/h, less than the govern value of 2.5 μSv/h for working place.

Unrealistic – The positioning technician needs sufficient time to position the next patient in the 30-min interval after the irradiated patient was removed.

2.8.2. Dose received from position the next patient

After removing the former patient, the residual dose rate in the treatment room was determined by the fixed components. The annual dose received by the positioning technician from positioning the next patient can be calculated by multiplying the total

number of patient positioning and the integral dose received from each positioning. We assumed that the time needed for the position process is 10 min and the patient began to enter the treatment room at 1-min cooling time. Then the annual dose received by the positioning technician from positioning the next patient can be calculated as shown in Table 10. In the calculation, for conservative calculation, the dose rate adopted that of #2 fixed-beam room with couch. From Table 10, the annual dose received by the technician from positioning is no more than 0.91 mSv/a. From Figs. 4 and 5, we observe that this value did not change much in the whole treatment room, except very close to the couch, which dominates the dose rate from fixed components in the distance of <1 m, and may reach 8 μSv/h at the isocenter and the saturation state. Hence, the distance to the couch should be carefully monitored during the positioning process.

3. Conclusions and suggestions

Through FLUKA's simulation and calculation of induced radioactivity in HJPMF's treatment room by activation formula, we found that the patient-induced radioactivity is a vital factor for radiation protection to patient escort and positioning technician. In HJPMF, only PBS mode will be used for treatment, but the results can be adopted to other proton medical facilities, as their treatment energies are almost the same as HJPMF, from tens of million electron volts to 250 MeV, and most of the induced radioactivity produced in nozzle and aperture from double scattering (DS) and uniform scanning (US) modes can be self-shielded by the components themselves. By analyzing the residual dose rate distribution and its decay with time, radionuclides' concentration and dose rate after a single short-time treatment and at saturation state, we confirmed that the patient-induced radioactivity dominates the radiation field in the treatment room between two treatments, which should be considered important for the procedure of proton therapy, but has been ignored for years.

In order to find the saturation activity at HJPMF's irradiation profile, new formulas for calculating the activity buildup process of periodic irradiation were derived and used to study the relationship between a nuclide's saturation degree and half-life. By comparing the 30-year continuous treating result and the periodic result, we found that the dose rate at 1-min cooling produced by fixed components from long-time treatment is at most 2.2 times of that from single short-time treatment, lower than expected, because the saturation degree of nuclides with middle and long half-lives has been degraded significantly by the short treating time and long cooling time. The buildup formulas and results are valuable and suitable to other accelerators too, as long as the irradiation profile is periodic (nested or not) or can be approximated as periodic.

To the patient, since his/her induced radioactivity may reach tens of micro-sievert per hour to 200 μSv/h, it is advised that at least 5-min cooling time for the main short-lifetime nuclide O-15 in the patient to decay, before the positioning technician enters the treatment room to remove the patient.

To the patient escort, the patient-induced radioactivity is not a serious problem, as the escort begins to contact the irradiated patient usually at 5 min after treatment finished or later, and the number of treatments for a patient is limited.

To the positioning technician, it is advised to pay attention to the contact distance and contact time of the irradiated patient, so as to reduce the dose received from removing the irradiated patient. It is also advised to pay attention to the induced radioactivity from couch (or other components), which is located near the isocenter and downside the beam direction, although its residual dose rate is one order of magnitude lower than patient, but more time is needed to position the next patient than to remove the irradiated patient. It is advised to have sufficient number of positioning technicians to reduce their average dose. Furthermore, it is notable that the dose from prompt radiation will make the acceptable dose from induced radioactivity lower than the annual dose limit. Therefore, regular monitoring of personal dose is very important.

It can be found that our results agree with Thomadsen's review paper (Thomadsen, 2014). It is advised to refer to this review paper for a comprehensive understanding of the induced radioactivity produced in various particle medical therapy facilities.

References

Barbier, M., 1969. Induced radioactivity. North-Holland Publishing Company,, Amsterdam.

Bohlen, T.T., Cerutti, F., Chin, M.P.W., Fasso`, A., Ferrari, A., Ortega, P.G., Mairani, A., Sala, P.R., Smirnov, G., Vlachoudis, V., 2014. The FLUKA code: developments and challenges for high energy and medical applications. Nucl. Data Sheets 120, 211–214.

Clement, C.H., 2012. Compendium of Dose Coefficients based on ICRP Publication 60, 119. ICRP Publication,.

Keith F. Eckerman and Jeffrey C. Ryman, External Exposure to Radionuclides in Air, Water, and Soil, Federal Guidance No. 12, EPA-402-R-93–081, 1993.

Alfredo Ferrari, Paola R. Sala, Alberto Fass_o, Johannes Ranft. Fluka manual: a multi-particle transport code (Program version 2011), GENEVA, 2011.

Laurie M. Unger* and D. K. Trubey, Specific Gamma-ray Dose Constants for Nuclides Important to Dosimetry and Radiological Assessment, ornl-rsic-45, May 1982.

Bhaskar Mukherjee, Radiation Shielding of a 230 MeV Proton Cyclotron for Cancer Therapy, Joint DESY and University of Hamburg Accelerator Physics Seminar, August 2009.

F. Stichelbaut, Radiation Sources in the Proteus 235 System, B0, 27/03/2014a.

F. Stichelbaut, Shielding Design for Hengjian Facility, 12/12/2014b.

Theis, C., Buchegger, K.H., Brugger, M., Forkel-Wirth, D., Roesler, S., Vincke, H., 2006. Interactive three dimensional visualization and creation of geometries for Monte Carlo calculations. Nucl. Instrum. Methods Phys. Res. A 562, 827–829.

Thomadsen, B., 2014. Potential hazard due to induced radioactivity secondary to radiotherapy: the report of task group 136 of the american association of physicists in medicine. Health Phys. 107 (5), 442-60.

Tokai-mura, Naka-gun, Ibaraki-ken, High Intensity Proton Accelerator Project (J-PARC) Technical Design Report Material & Life Science Experimental Facility [J]. JEARI-Tech-2004–001-part2, 878–882.

Wu, Qingbiao, 2014. Study on Induced Radioactivity of China Spallation Neutron Source (doctoral dissertation, April). The University Of Chinese Academy Of Sciences (CAS),.